Quantitative investigation of calcimimetic R568 on beta cell adhesion and mechanics using AFM single-cell force spectroscopy

Article *in* FEBS Letters · April 2014

DOI: 10.1016/j.febslet.2014.02.058

CITATIONS
21

READS
146

5 authors, including:

Eleftherios Siamantouras
The University of Warwick
26 PUBLICATIONS **403** CITATIONS
SEE PROFILE

Claire E Hills
University of Lincoln
84 PUBLICATIONS **1,936** CITATIONS
SEE PROFILE

Mustafa Y. G. Younis
University of Benghazi
35 PUBLICATIONS **183** CITATIONS
SEE PROFILE

Paul Squires
University of Lincoln
125 PUBLICATIONS **4,024** CITATIONS
SEE PROFILE

FEBS Letters 588 (2014) 1178–1183

journal homepage: www.FEBSLetters.org

Quantitative investigation of calcimimetic R568 on beta cell adhesion and mechanics using AFM single-cell force spectroscopy

Eleftherios Siamantouras [a], Claire E. Hills [b], Mustafa Y.G. Younis [b], Paul E. Squires [b], Kuo-Kang Liu [a,*]

[a] School of Engineering, University of Warwick, CV4 7AL, UK
[b] School of Life Sciences, University of Warwick, CV4 7AL, UK

ARTICLE INFO

Article history:
Received 20 December 2013
Revised 14 February 2014
Accepted 24 February 2014
Available online 5 March 2014

Edited by Lukas Huber

Keywords:
AFM-SCFS
Cell adhesion
Indentation
Elasticity
CaSR
Calcimimetic

ABSTRACT

In this study we use a novel approach to quantitatively investigate mechanical and interfacial properties of clonal β-cells using AFM-Single Cell Force Spectroscopy (SCFS). MIN6 cells were incubated for 48 h with 0.5 mM Ca^{2+} ± the calcimimetic R568 (1 μM). AFM-SCFS adhesion and indentation experiments were performed by using modified tipless cantilevers. Hertz contact model was applied to analyse force–displacement (*F–d*) curves for determining elastic or Young's modulus (*E*). Our results show CaSR-evoked increases in cell-to-cell adhesion parameters and *E* modulus of single cells, demonstrating that cytomechanics have profound effects on cell adhesion characterization.

1. Introduction

The role of the calcium-sensing receptor CaSR in the systemic circulation is to sense changes in extracellular Ca^{2+} and evoke appropriate counter-regulatory responses to regain normocalcaemia [4]. The functional link between the receptor and regulation of systemic calcium in normal physiology and disease has been extensively studied [4]. However, CaSR expression is not restricted to the cells involved in the control of systemic Ca^{2+} [5]. It has been well recognized that CaSR activation affects function in disparate tissue types, including pancreatic beta-cells [29,12,19,21].

Epithelial (E)-cadherin is a surface adhesion protein involved in tethering adjacent cells and ensuring close cell–cell interaction. E-cadherin ligation mediates beta-cell-to-beta-cell coupling and regulates intercellular communication within islets [3]. A study by Rogers et al. [27] suggested that E-cadherin mediated cell adhesion contributes to the enhanced secretory function of beta-cell clusters. Neutralization of E-cadherin reduced glucose-evoked synchronicity in calcium signals between adjacent cells and reduced insulin secretion [27]. These data imply that E-cadherin mediated cell adhesion has important repercussions for the islet function in terms of glucose responsiveness and insulin secretion.

We have previously demonstrated that the activation of CaSR using the calcimimetic R568, increased the expression of E-cadherin, which in turn increased functional tethering between beta-cells [15]. In the current study we quantitatively monitored changes in cell elasticity induced by activation of the CaSR by the calcimimetic R568. Atomic Force Microscopy based Single Cell Force Spectroscopy (AFM-SCFS) was used to perform cell-to-cell adhesion and single cell indentation experiments. The SCFS system incorporates an improved positioner to allow for longer displacement measurements up to 100 μm for separating two adherent cells, in a high force resolution (∼pN) over a large dynamic range (∼5 pN to ∼100 nN). This system provides sufficient force and displacement ranges to ensure accurate detection of maximum unbinding force of ligand-receptor interactions in cell-to-cell adhesion measurement [2,26,9,14], while it has been used extensively for studying cadherin mediated adhesion [1,25,22]. In the current study the instrument was also fitted with a spherical bead-attached cantilever beam to indent single cells and thereby calculate cell elasticity, i.e. Young's modulus, from the measured force–displacement curves using Hertzian contact model [32]. The novel use of this improved AFM-SCFS system permits us to examine cellular adhesion, tethering of cells and cell elasticity and more importantly to elucidate the intricate interplay between these factors.

* Corresponding author. Address: School of Engineering, University of Warwick, Coventry CV4 7AL, UK.
E-mail address: I.K.Liu@warwick.ac.uk (K.-K. Liu).

http://dx.doi.org/10.1016/j.febslet.2014.02.058
0014-5793/

2. Materials and methods

2.1. Materials

MIN6 cells were obtained from Dr. Y. Oka and J.-I. Miyazaki (Univ. of Tokyo, Japan). Fibronectin, Dulbecco's Modified Eagles Medium (DMEM), Hams-F12, glutamine, penicillin-streptomycin and phosphate buffered saline (PBS) were from Sigma–Aldrich (Poole, Dorset, UK). The calcimimetic R568 was from Amgen Inc. (Thousand Oaks, CA, USA). Tissue culture plastic-ware was from Invitrogen Life Technologies (Paisley, UK).

2.2. Maintenance of MIN6 cells

MIN6 cells (passage 35–40) were maintained at 37 °C in a humidified atmosphere of 5% CO_2 in air in DMEM supplemented with 15% FCS, glutamine (2 mM) and penicillin/streptomycin (100 U/ml/0.1 mg/ml). Prior to treatment, cells were seeded onto 40 mm petri-dishes and serum starved overnight. Cells were then placed for 48 h in DMEM containing both low glucose (5 mM) and low calcium (0.5 mM) +/− the calcimimetic R568 (1 μM) [15]. Suspended (free) cells were prepared under identical conditions before being physically scrapped off the T25 flasks with gentle agitation and re-suspended in fresh DMEM.

2.3. Atomic Force Microscopy

Experiments were performed using the CellHesion®200 module (JPK Instruments, Germany) installed on an Eclipse TE 300 inverted microscope (Nikon, USA). During each experiment, cells were maintained at 37 °C using a BioCell™ temperature controller (JPK Instruments, Berlin, Germany). All experiments were performed in CO_2 – independent media. Phase microscopy images were acquired using a CCD camera connected on the side port of the microscope. The entire set-up was supported on an anti-vibration table (TMC 63-530, USA).

Tip-less silicon nitride cantilevers (Arrow TL-1, NanoWorld, Switzerland), with force constant 0.03 N/m, were used for conducting cell-to-cell adhesion and single cell indentation experiments. The actual spring constant of the cantilever was determined before experiments by using the manufacturer's software (JPK instruments, Germany) based on the thermal noise method [17]. Since the resonance of soft cantilevers in fluid is much lower and very susceptible to noise a correction factor of 0.251 was used [6].

2.4. Cell-to-cell adhesion experiments

The tip-less cantilevers were chemically functionalized for a single suspended cell to be attached. Initially the cantilevers were sterilised by UV treatment (15 min), before being incubated in poly-L-lysine (25 μg/ml in PBS, 30 min, RT) and then fibronectin (20 μg/ml in PBS, 2 h, 37 °C) [16]. After functionalization cantilevers were stored in PBS solution at 4 °C and used within 3 days. To record a force curve for calibration, the cantilever was configured to approach the base of a cell-free petri-dish once, to minimize the loss of coating (set-point 2 V). Suspended cells were dispensed into the petri dish using a pipette. Free cells stick on the substrate within 5 min, hence the cell-cantilever attachment procedure was performed rapidly (2 min). With the aid of optical microscope the cantilever was pressed against a single free cell by performing a force curve. The set-point force and contact time was 0.8 nN and 5 s, respectively. During the contact period, the instrument was set in a constant force mode, in which force is kept constant by adjustments of the piezo-actuator height. Once a single cell was attached to the cantilever, it was left to recover for at least 5 min to form strong binding with the functionalized surface [11].

The cantilever-attached cell was brought in contact with another cell adhering on the substrate, until a preset contact force of 0.8 nN was reached. The cells remained in contact for 5 s, in which surface bonding was formed. Next, the cantilever was retracted and force versus displacement measured until the two cells were completely separated. The procedure was repeated three times for each cell tested, with 30 s intervals between each measurement. The attached cell was used to perform measurements on approximately 3–5 cells for each dish, using multiple dishes from at least 3 separate samples of cells in each experiment ($n = 3$).

2.5. Cell indentation experiments

Using a small amount of two-part fast setting epoxy glue (5 min), colloidal probes were prepared by gluing an 11 μm polystyrene microsphere (Polybeads®, Polysciences, USA) on a tipless TL-1 cantilever. The attachment procedure was performed on the stage of AFM with the aid of the inverted optical microscope. The microsphere was attached immediately by performing an approach curve directly above the sphere. Fig. 1(a) shows optical images of polymeric bead attached to a tipless cantilever.

Each substrate cell was indented 5 times with an interval pause of 60 s, while force–displacement (F–d) curves were recorded simultaneously. For consistency, all cells were indented immediately

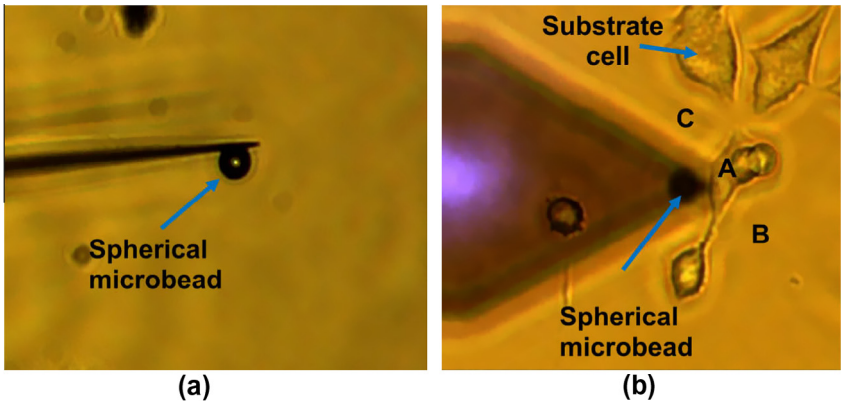

Fig. 1. (a) An optical image showing the side view of a 10 μm silica microsphere attached to the end of an arrow TL1 tipless cantilever. (b) An optical image showing the top view of the cantilever-bead and MIN6 cells on the substrate. The determination of cell height prior indentation experiments is also demonstrated; a low set-point force (0.2 nN) was used for the AFM cantilever to touch a point in a clean area, such as B and C, next to a measured cell (A area). The displacement difference between B (or C) and A was used to determine the height of the cell.

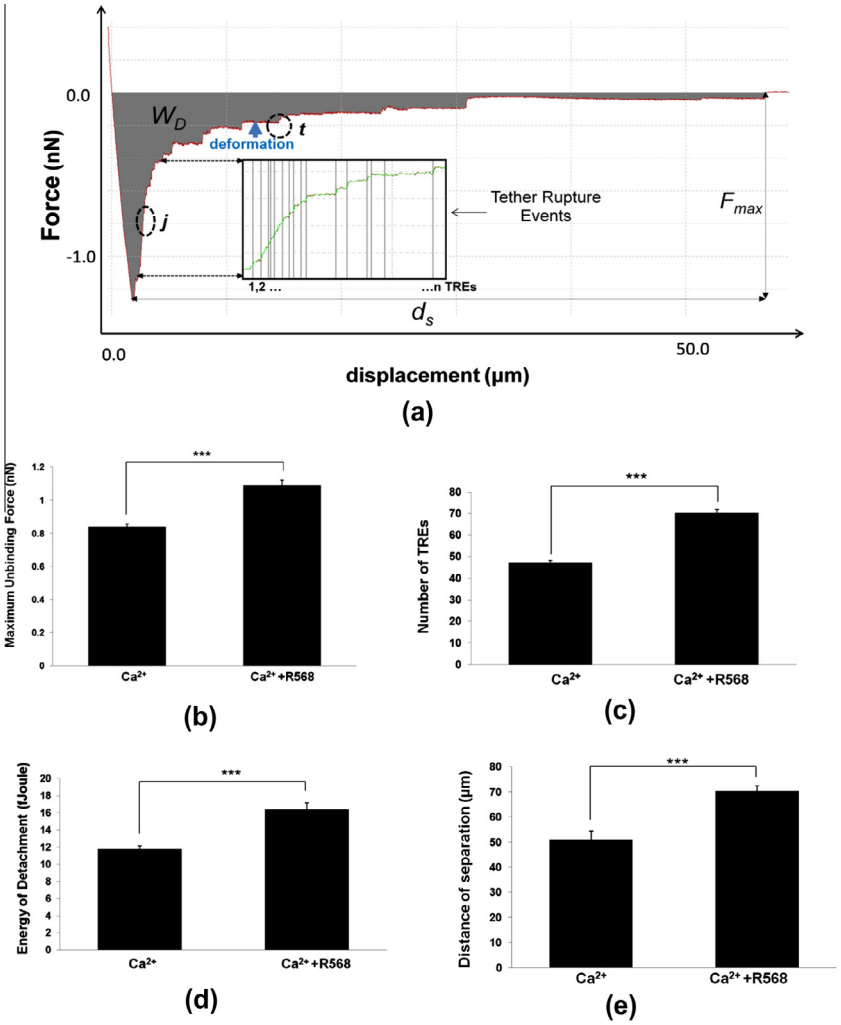

Fig. 2. (a) Example of a retraction force–distance curve obtained by cell-to-cell adhesion measurement. F_{max} is the difference between the minimum force value and the baseline, while W_D (grey region) is the integral of the continuous area under the baseline. Next, d_s can be determined by the difference of displacements between F_{max} and the point of complete separation. Unbinding of ligations during the pulling phase mainly falls in two areas, those events in which a ramp in the deflection of the cantilevers is preceded ('*j*' events) and those which a deformation of membrane tethering is preceded ('*t*' events). Zooming in the *x*-axis displays detection of the number of early TREs. The effects of the calcimimetic R568 (1 µM) on (b) the maximum unbinding force F_{max} (increased by 30%), (c) the number of tethering rupture events (TREs) increased by 48%, (d) the energy of detachment W_D (increased by 39%) and (e) the distance to complete separation (increased by 37%) are shown. Data are expressed as mean ± S.E.M. of 10–12 cells from 3 separate experiments, where key significances are shown, $^{***}P < 0.001$.

above the nucleus. To determine height of the cell, approach curves with low set-point (0.2 nN) were performed in the area surrounding the cell and on its surface. The height of each cell was calculated by their displacement difference, as illustrated in Fig. 1(b). Since, the indentation depth was pre-determined for each cell, indentation experiments were performed to measure the force–displacement curves up to the pre-set indentation depth, according to the height measurement of the cell. Approach and retraction speed was kept constant at 5 µm/s to minimize hydrodynamic forces acting on the cantilever [10].

2.6. Theoretical model

Force–displacement curves acquired by indentation experiments were analyzed using Hertz model. When a cell is indented by a spherical probe, the force *F* applied on the cell was determined as function of indentation depth δ as follows,

$$F = \frac{E}{1-\nu^2}\left[\frac{a^2+R_S^2}{2}\ln\frac{R_S+a}{R_S-a} - aR_S\right] \quad \text{(eq.1)}$$

$$\delta = \frac{a}{2}\ln\frac{R_S+a}{R_S-a} \quad \text{(eq.2)}$$

where E and ν are the Young's Modulus and Poisson's ratio of the cell respectively, α is the radius of probe-cell contact circle, and R_S is the radius of the spherical probe.

The Hertz model is only valid for indentations up to 10% of the samples height, where substrate effects are considered insignificant [7]. To meet such a criterion, all the force–displacement curves obtained from cell indentation experiments were fitted in the range of 5–10% of the height of each cell. The Poisson's ration was set to 0.5 in the study, since this value is generally accepted for soft biological cells [24].

2.7. Data analysis

To process all force–displacement curves the JPK Data analysis software was used. To signify statistical differences data were evaluated using a paired *t*-test. Data are expressed as mean ± SEM. and '*n*' shows number of experiments. $P < 0.05$ was taken to indicate statistical significance.

3. Results

A few sets of measurements were performed to confirm the selected parameters for adhesion measurements. Using identical experimental specifications 10–12 cells were examined and the results are shown in Fig. 3. Retraction force–displacement (F–d) curves provide important information regarding the adhesion between two cells, such as the energy of detachment W_D, the maximum unbinding force F_{max}, the distance of complete separation d_s, and the number of tethering rupture events (TREs) (Fig. 2(a)). The determination of the point at which the cells are completely separated represents the x-axis baseline, which acts as a reference for further analysis. The unbinding force is the force required to break the ligation bonding between E-cadherin on coupled cells, whilst the energy of detachment is the total energy that is consumed until the two cells are completely detached. The pulling length from the highest negative deflection of the cantilever and the point of complete separation represents the distance of complete separation d_s between two cells. Retraction F–d curves acquired during cell-to-cell adhesion experiments typically exhibit a step-like pattern resulting from the rupture of surface ligations. Number of TREs can be detected by identifying sharp steps of force that correspond to bond ruptures [20]. In the early part of the retraction curve complex unbinding events occur ('j' events) that are preceded by a force ramp, while as the pulling distance increases a plateau in the displacement indicates that membrane tethering extrudes rupture of ligation ('t' events) [11]. The results indicate that the calcimimetic R568 (1 μM) increased the number of tether rupture events by 48%, resulting in an increase of the maximum unbinding force by 30%. However, the detachment energy was increased more significantly by 39%, consistent with the detachment distance increasing by 37% (10–12 cells, $n = 3$, $P < 0.001$) (Fig. 2(b–e)).

A typical indentation F–d curve for investigating the elastic properties of single cells is shown in Fig. 3(a). By applying the Hertz model for elastic indentation to F–d curves recorded during indentation, information about the local elastic or Young's modulus (E) was extracted. The contact point is defined as the point where cantilever deflection starts to rise and in fact accurate determination of the contact point is crucial for a reliable calculation of the elastic modulus. By fitting discrete parts of the extension curve to the model, the point where the probe is in contact with the plasma membrane can be identified. Fig. 3(b) shows a histogram of elastic modulus E determined from the F–d curves measured on a central region above the nucleus of cells. More than 100 curves were analysed and the average calculated value of E for the control cells is 503 Pa while for the treated cells is 331 Pa. The results indicate that the calcimimetic R568 (1 μM) decreased the elastic modulus by 34% (30 cells, $n = 3$, $P < 0.001$) (Fig. 4).

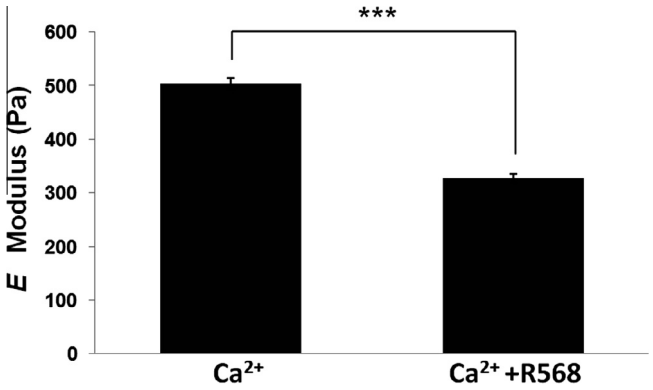

Fig. 4. The effects of calcimimetic R568 (1 μM) on the elastic modulus (decreased by 54%). Data are expressed as mean ± S.E.M. of at least 30 cells from 3 separate experiments, where key significances are shown, $^{***}P < 0.001$.

To further assess the effects of viscoelastic deformation on cell-to-cell adhesion, F–d curves were performed with incremental pulling or separation speed. Due to the soft nature of the cells, data were analysed up to a speed of 12.5 μm/s, since a significantly higher displacement range than 100 μm was required for higher velocities. The results demonstrate a tenfold increase of the W_D in comparison to the F_{max} as the pulling speed increases, up to the pulling distance of 100 μm (10–12 cells, $n = 3$) (Fig. 5(a and c)). The decrease in the number of TREs for a displacement range of 30 μm after F_{max} was two times higher for the cells treated with the calcimimetic in comparison to the untreated. Fig. 6 shows respectively that for both control and treated cells, F_{max} is dependent on velocity, based on Eq. (eq. 3), which is derived from the Bell–Evans model [28,23].

$$F_i \sim f_\beta \ \ln(\text{loading rate}) + \text{constant} \qquad \text{(eq.3)}$$

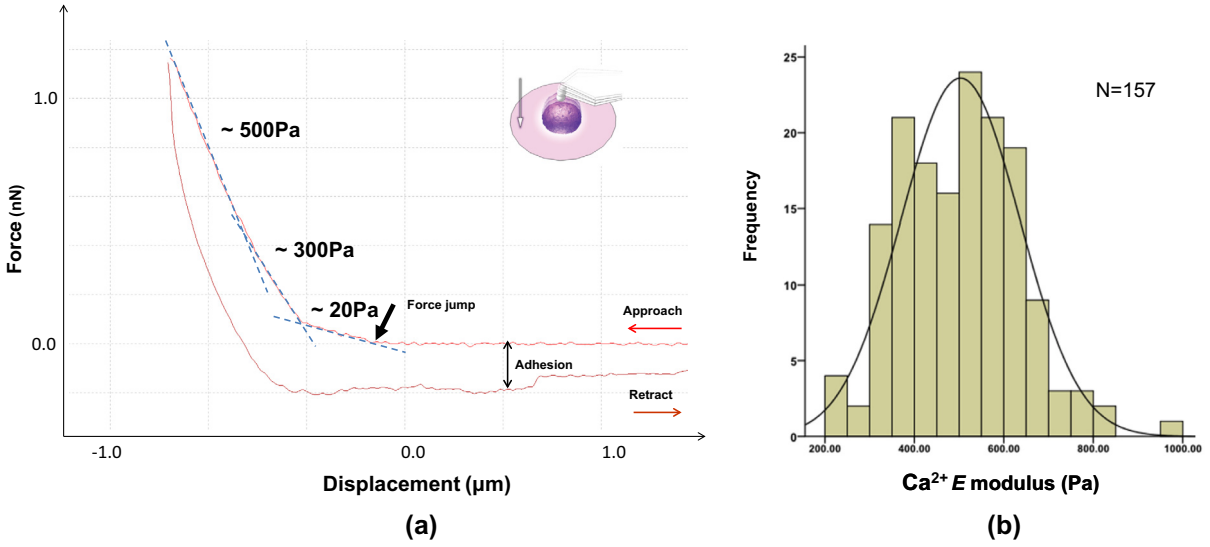

Fig. 3. (a) A typical force displacement curve obtained by a nanoindentation measurement. Elasticity can be calculated by fitting Hertz model into the extended part of the curve, in which adhesion is negligible. (b) A histogram of elastic modulus E obtained from the F–d curve measurements of MIN6 cells measured on a central region.

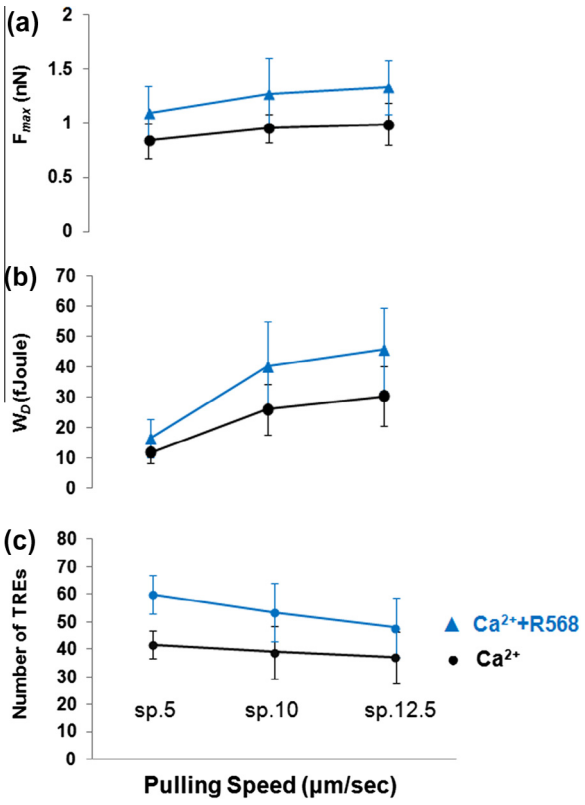

Fig. 5. Effects of increasing pulling speed on (a) maximum unbinding force F_{max}, (b) work of detachment W_D and (c) number of tethering rupture events TREs.

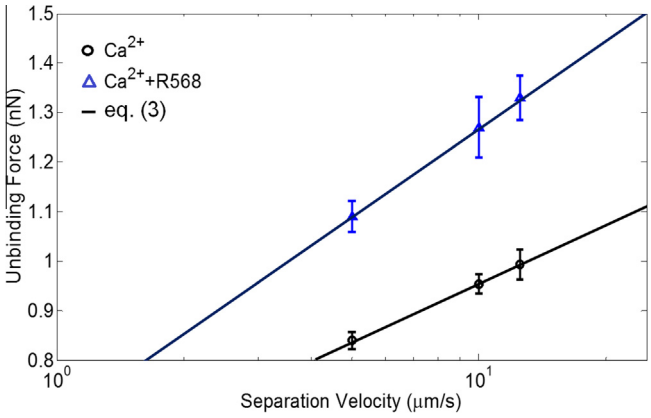

Fig. 6. Dependence of unbinding forces on separation velocities of Ca^{2+} and Ca^{2+}+R568 treated beta-cells.

where F_i is the unbinding force and f_β is the characteristic force scale over the single energy barrier until the complete separation of the surface ligation.

4. Discussion

Extracellular calcium promotes the interaction between the extracellular domains of E-cadherin on adjacent cells, whilst the intracellular domain of the trans-membrane protein binds to β-catenin, α-catenin and the actin cytoskeleton. Ligation of E-cadherin to a partner protein on an adjacent cell, stimulates other down-stream cytoskeletal-binding proteins including the phosphoinositide 3-kinase PI3K [31]. In keratinocytes it was suggested that the CaSR was involved in regulating calcium stimulated formation of the E-cadherin complex [30]. Our previous results suggest that the activation of the receptor improves β-cell function by increasing cell adhesiveness through enhanced expression of E-cadherin and via PI3K-dependent cytoskeletal reorganisation [15]. Under appropriate conditions MIN6 cells grow as 3-dimensional cell clusters known as pseudoislets [13]. Analysis of whole cell protein suggested that CaSR expression is higher in monolayers compared to pseudoislets [19]. As adhesion and indentation experiments are only possible on monolayers, and due to the fact that CaSR expression is greater in this type of cell configuration, all experiments were performed on monolayers.

Surface protein binding affinity was responsible for the increase in F_{max}, however our results suggest that this was only partially responsible for the increase in W_D, which was influenced by the changes in the elastic mechanical properties of the cell. An increase in W_D could mirror changes in the compliance of cells, since W_D is partly contributed from the elastic deformation of an elastic sphere apart from the adhesion due to surface contact [18]. This is clearly demonstrated by the increase in E as well as by the dramatic increase of W_D when pulling speed was increased. The comparison between increasing pulling speeds suggests that although the surface properties were significant for changes in F_{max}, changes in the mechanical properties in response to cytoskeletal reorganization, rather than ligation binding affinity or surface density of E-cadherin, contribute to the dramatic changes of the W_D. The larger decrease of the treated cells' TREs also implies that fewer bindings were ruptured over the same distance of separation, due to their higher compliance. Moreover, the increase in F_{max} with increased pulling speed could be contributed to the viscoelastic deformation of the surface proteins themselves and membrane tethers. Diz-Muñoz et al. [8] measured the dynamics of tethering force between the AFM tip and cell membrane, also concluding that the unbinding force increased as the separation speed increased. Both our adhesion and indentation measurements clearly suggest that the viscoelastic deformation has a significant influence on the adhesion energy between two adherent cells and that cytomechanics contribute to the E-cadherin mediated adhesion in our system.

5. Conclusion

In the current study we have investigated the effects of whole cell elasticity under the influence of the calcimimetic R568 in the MIN6 clonal β-cell line and we have provided quantitative evidence that the mechanical properties of cells have an effect on cell-to-cell interaction. Activation of CaSR increases the expression of the surface adhesion protein E-cadherin [15], whilst affecting the intracellular domain of the protein by increasing the elasticity of the cell. The changes in the inner mechanical properties of the cells had a strong effect on cell-to-cell adhesion energy, mainly due to viscoelastic deformation. As a consequence, adhesion parameters were altered not only due to biomolecular changes in cell surface expression of E-cadherin, as previously reported, but also due to changes in the biomechanical properties of the cells. Therefore, in improving beta cell function, activation of CaSR not only increases E-cadherin expression and cell-to-cell adhesiveness but it also initiates &/or modulates intracellular signalling of the F-actin cytoskeleton via the catenins. The net result is a change in the mechanistic behaviour of whole cell.

Acknowledgements

This work was supported by grants from Diabetes UK (BDA: 09/0003913, and 12/0004546) and Leverhulme Trust (PRG-2012-738).

The authors are grateful to Amgen Inc. for their supply of the calcimimetic R568 and JPK instrument for their technical support in the use of single-cell force spectroscopy.

References

[1] Baumgartner, W. (2000) Cadherin interaction probed by atomic force microscopy. Proc. Natl. Acad. Sci. USA 97 (8), 4005–4010.
[2] Benoit, M. et al. (2000) Discrete interactions in cell adhesion measured by single-molecule force spectroscopy. Nat. Cell Biol. 2 (6), 313–317.
[3] Brereton, H.C. et al. (2006) Homotypic cell contact enhances insulin but not glucagon secretion. Biochem. Biophys. Res. Commun. 344 (3), 995–1000.
[4] Brown, E.M. (2007) Clinical lessons from the calcium-sensing receptor. Nat. Clin. Pract. Endocrinol. Metab. 3 (2), 122–133.
[5] Brown, E.M. and MacLeod, R.J. (2001) Extracellular calcium sensing and extracellular calcium signaling. Physiol. Rev. 81 (1), 239–297.
[6] Butt, H.-J. and Jaschke, M. (1995) Calculation of thermal noise in atomic force microscopy. Nanotechnology 6 (1), 1–7.
[7] Dimitriadis, E.K. et al. (2002) Determination of elastic moduli of thin layers of soft material using the atomic force microscope. Biophys. J. 82 (5), 2798–2810.
[8] Diz-Muñoz, A. et al. (2010) Control of directed cell migration in vivo by membrane-to-cortex attachment. PLoS Biol. 8 (11), e1000544.
[9] Franz, C.M. et al. (2007) Studying integrin-mediated cell adhesion at the single-molecule level using AFM force spectroscopy. Sci. STKE 406, l5.
[10] Franz, C.M. and Puech, P.-H. (2008) Atomic force microscopy: a versatile tool for studying cell morphology, adhesion and mechanics. Cell. Mol. Bioeng. 1 (4), 289–300.
[11] Friedrichs, J. et al. (2010) Quantifying cellular adhesion to extracellular matrix components by single-cell force spectroscopy. Nat. Protoc. 5 (7), 1353–1361.
[12] Gray, E. et al. (2006) Activation of the extracellular calcium-sensing receptor initiates insulin secretion from human islets of Langerhans: involvement of protein kinases. J. Endocrinol. 190 (3), 703–710.
[13] Hauge-Evans, A.C. et al. (1999) Pancreatic beta-cell-to-beta-cell interactions are required for integrated responses to nutrient stimuli: enhanced Ca2+ and insulin secretory responses of MIN6 pseudoislets. Diabetes 48 (7), 1402–1408.
[14] Helenius, J. et al. (2008) Single-cell force spectroscopy. J. Cell Sci. 121 (Pt 11), 1785–1791.
[15] Hills, C.E. et al. (2012) Calcium-sensing receptor activation increases cell–cell adhesion and β-cell function. Cell. Physiol. Biochem. 30 (3), 575–586.
[16] Hills, C.E. et al. (2013) "Special k" and a loss of cell-to-cell adhesion in proximal tubule-derived epithelial cells: modulation of the adherens junction complex by ketamine. PLoS One 8 (8), e71819.
[17] Hutter, J.L. and Bechhoefer, J. (1993) Calibration of atomic-force microscope tips. Rev. Sci. Instrum. 64 (7), 1868–1873.
[18] Johnson, K.L. and Greenwood, J.A. (1997) An adhesion map for the contact of elastic spheres. J. Colloid Interface Sci. 192 (2), 326–333.
[19] Jones, P.M. et al. (2007) Expression and function of the extracellular calcium-sensing receptor in pancreatic beta-cells. Arch. Physiol. Biochem. 113 (3), 98–103.
[20] Kerssemakers, J.W.J. et al. (2006) Assembly dynamics of microtubules at molecular resolution. Nature 442 (7103), 709–712.
[21] Kitsou-Mylona, I. et al. (2008) A role for the extracellular calcium-sensing receptor in cell–cell communication in pancreatic islets of langerhans. Cell. Physiol. Biochem. 22 (5–6), 557–566.
[22] Leckband, D. and Sivasankar, S. (2012) Biophysics of cadherin adhesion. Curr. Opin. Cell Biol. 24 (5), 620–627.
[23] Lo, Y.S. et al. (2001) Loading-rate dependence of ligand-receptor bond-rupture forces studied by atomic force microscopy. Langmuir 17 (12), 3741–3748.
[24] Mahaffy, R.E. et al. (2004) Quantitative analysis of the viscoelastic properties of thin regions of fibroblasts using atomic force microscopy. Biophys. J. 86 (3), 1777–1793.
[25] Panorchan, P. et al. (2006) Single-molecule analysis of cadherin-mediated cell–cell adhesion. J. Cell Sci. 119 (Pt 1), 66–74.
[26] Puech, P.-H. et al. (2006) A new technical approach to quantify cell-cell adhesion forces by AFM. Ultramicroscopy 106 (8–9), 637–644.
[27] Rogers, G.J. et al. (2007) E-cadherin and cell adhesion: a role in architecture and function in the pancreatic islet. Cell. Physiol. Biochem. 20 (6), 987–994.
[28] Strunz, T. et al. (1999) Dynamic force spectroscopy of single DNA molecules. Proc. Natl. Acad. Sci. USA 96 (20), 11277–11282.
[29] Squires, P.E. et al. (2000) The extracellular calcium-sensing receptor on human beta-cells negatively modulates insulin secretion. Diabetes 49 (3), 409–417.
[30] Tu, C.-L. et al. (2008) Inactivation of the calcium sensing receptor inhibits E-cadherin-mediated cell–cell adhesion and calcium-induced differentiation in human epidermal keratinocytes. J. Biol. Chem. 283 (6), 3519–3528.
[31] Vaezi, A. et al. (2002) Actin cable dynamics and Rho/Rock orchestrate a polarized cytoskeletal architecture in the early steps of assembling a stratified epithelium. Dev. Cell 3 (3), 367–381.
[32] Vinckier, A. and Semenza, G. (1998) Measuring elasticity of biological materials by atomic force microscopy. FEBS Lett. 430 (1–2), 12–16.